Breakpoint Characterization of the der(19)t(11;19)(q13;p13) in the Ovarian Cancer Cell Line SKOV-3

Wiebke Onkes,[1] Regina Fredrik,[1] Francesca Micci,[2,3] Benjamin J Schönbeck,[4] Jose I Martin-Subero,[5] Reinhard Ullmann,[6] Felix Hilpert,[1] Karen Bräutigam,[7] Ottmar Janssen,[4] Nicolai Maass,[7] Reiner Siebert,[8] Sverre Heim,[2,3] Norbert Arnold,[1] and Jörg Weimer[1]*

[1]Department of Obstetrics and Gynaecology, University Medical Center Schleswig-Holstein, Christian-Albrechts University, Kiel, Germany
[2]Section for Cancer Cytogenetics, Institute for Medical Informatics, The Norwegian Radium Hospital, Oslo University Hospital, Oslo, Norway
[3]Centre for Cancer Biomedicine, Institute for Clinical Medicine, Faculty of Medicine, University of Oslo, Norway
[4]Molecular Immunology, Institute of Immunology, University Medical Center Schleswig-Holstein, Kiel, Germany
[5]Department of Anatomic Pathology, Pharmacology and Microbiology, University of Barcelona, Barcelona, Spain
[6]Department Human Molecular Genetics, Max Planck Institute for Molecular Genetics, 14195 Berlin, Germany
[7]Department of Gynecology and Obstetrics, University Medical Center RWTH, Aachen, Germany
[8]Institute of Human Genetics, University Hospital Schleswig-Holstein, Campus Kiel/ University Kiel, Germany

About 20% of ovarian carcinomas show alterations of 19p13 and/or 19q13 in the form of added extra material whose origin often is from chromosome 11. Based on earlier spectral karyotype analysis of the ovarian cancer cell line SKOV-3, which shows an unbalanced translocation der(19)t(11;19), the aim of this study was to determine the precise breakpoints of that derivative chromosome. After rough delimitation of the breakpoints of microdissected derivative chromosomes by array analysis, we designed a matrix of primers spanning 11q13.2 and 19p13.2 detecting multiple amplicons on genomic and cDNA. Sequencing the amplicons, accurate localization of both breakpoints on both chromosomes was possible and we found that exon 14 of *HOOK2* from chromosome 19 and exon 2 of *ACTN3* from chromosome 11 were fused in the derivative chromosome. The breakpoint in the *HOOK2* gene was in an intrinsic triplet of nucleic acids leading to a shift in the *ACTN3* reading frame in the derivative chromosome. This frameshift alteration should give rise to an early stop codon causing a loss of function of ACTN3. Signals in two-dimensional Western blotting exactly match to calculated molecular mass and the isoelectric point of the fusion protein.

INTRODUCTION

Ovarian carcinoma is the second most common cancer in the female reproductive tract. Because of its vague and belated symptoms, diagnosis is usually late leading to a high mortality rate. More than 400 karyotypically characterized ovarian carcinomas are listed in the cytogenetic literature (Mitelman et al., 2012). In general, simple numerical chromosomal aberrations, such as trisomy 12, are common in borderline or well-differentiated carcinomas (Jenkins et al., 1993; Pejovic, 1995), whereas complex changes, including losses, gains, unbalanced translocations, and additional material of unknown origin in derivative chromosomes, are typical of poorly and moderately differentiated carcinomas. Alterations of 19p13 and 19q13 in the form of added extra material are among the most frequent findings (Pejovic et al., 1989, 1992; Jenkins et al., 1993; Thompson et al., 1994b; Micci et al., 2009, 2010). Although some authors favor the region 19q13 being responsible for tumor genesis anyway (Whang-Peng et al., 1984; Bello and Rey, 1990; Thompson et al., 1994a; Guan et al., 1995), Micci et al. (2009, 2010) have studied 37 derivative chromosomes from 26 ovarian carcinomas using FISH-MD and array-painting detecting two regions of primary interest on 19p: one spanning from 20.80 Mbp to 20.85 Mbp and another more distal in 19p13.2. They also pointed out that a particularly common donor of added material could be traced back to

Supported by: Deutsche Forschungsgemeinschaft (AZ AR 262/1-1) and the state of Schleswig-Holstein.

*Correspondence to: Jörg Weimer, UKSH, Campus Kiel; Klinik für Gynäkologie und Geburtshilfe; Arnold-Heller Str. 3, Haus 24; 24105 Kiel, Germany. E-mail: jweimer@email.uni-kiel.de

Received 7 August 2012; Accepted 4 January 2013

DOI 10.1002/gcc.22048

Published online 30 January 2013 in Wiley Online Library (wileyonlinelibrary.com).

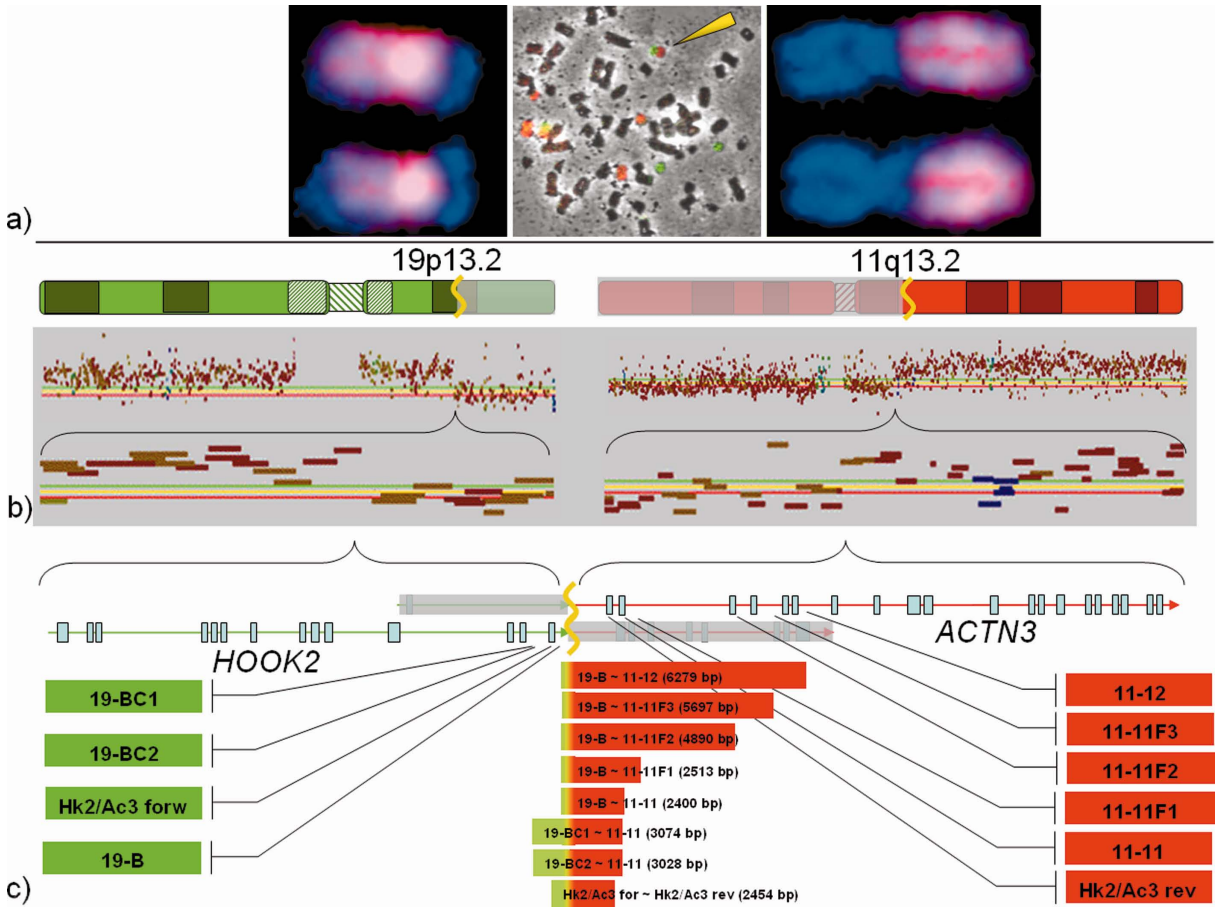

Figure 1. PCR walking confirms the position of the fusion in the derivative chromosome der(19)t(11;19)(q13.2;p13.2) preanalyzed by microdissection and array painting. A: A SKOV-3 metaphase is shown in the middle. The derivative chromosome der(19)t(11;19)(q13.2;p13.2) isolated by microdissection (indicated by a yellow arrow) has been identified by colocalized fluorescence signals from chromosome 19 labeled in green and from chromosome 11 labeled in red. Next to this metaphase, the reverse painting signals onto normal chromosomes reveal the composition of this derivative chromosome. B: The breakpoint region is further delineated by array painting of labeled DNA from the isolated derivative chromosome onto a 32 K BAC array being relatively placed to its corresponding position. C: the exact breakpoint in the fusion region within the *HOOK2* gene on chromosome 19 and within the *ACTN3* gene on chromosome 11 is proved by PCR walking. The primers (green and red boxes) are shown in the context of the exons of each gene (blue bars). The boxes with a color gradient from green to red represent the PCR products from genomic DNA demonstrating their starting and ending point as well as their relative length. [Color figure can be viewed in the online issue, which is available at wileyonlinelibrary.com.]

chromosome arm 11q as seen first by Pejovic et al. (1991, 1992).

Against the background of these findings and those reached in previous analysis of the ovarian cancer cell line SKOV-3 by spectral karyotyping analysis followed by derivative chromosome microdissection and reverse painting (Weimer et al., 2008; Fig. 1), we have already described a recurrent translocation and the presence of a der(19)t(11;19)(q13.2;p13.2). Therefore in this study, we focused on determining the precise breakpoints of this derivative chromosome through PCR walking and sequencing. Knowing the involved genes could offer new insights about ovarian carcinogenesis and may eventually lead to targeted therapy.

MATERIALS AND METHODS

Cell Culture

The human ovarian adenocarcinoma cell line SKOV-3 was obtained from the American Type Culture Collection (Manassas, VA). Cells were cultured in RPMI-1640 medium (Biochrom, Berlin, Germany) supplemented with 10% fetal calf serum (Gibco/Invitrogen, Karlsruhe, Germany), 10,000 U/ml penicillin (Biochrom) and 10,000 µg/ml streptomycin (Biochrom). They were incubated at 37°C in a humidified atmosphere containing 5% CO_2 and dissociated by trypsin-EDTA after growth to 80% confluence. The authenticity of the cell line SKOV-3 was verified by short tandem repeat finger print analysis using

the AmpFλSTR® Identifiler® PCR Amplification Kit (Applied Biosystems, Foster City, CA) and compared with the database of DSMZ in Braunschweig, Germany.

Breakpoint Pre-Localization by FISH-MD and Reverse Painting

Initial information about relevant primer positioning was generated by isolation of the der(19)t(11;19) from SKOV-3 by chromosome microdissection and amplification of isolated DNA by DOP-PCR (Weimer et al., 2000). The amplified DNA was hybridized on normal chromosomes and, in order to get higher resolution, on a 32K BAC-tile array (Fig. 1) as well as on a custom HD-CGH Microarray (4x44k) (Agilent Technologies, Böblingen, Germany). The signal edges gave information about the involved breakpoint. The primers of the matrix were positioned so that their product would cross the breakpoint from one chromosome to the other.

Genomic PCR-Matrix of Chromosome 11 and Chromosome 19

250 ng of DNA extracted from SKOV-3 by DNeasy Tissue Kit (QIAGEN, Hilden, Germany) was utilized for long range PCR with the Expand Long Template PCR System (Roche Diagnostics, Mannheim, Germany). A series of 12 primers on chromosome 11 and 10 primers on chromosome 19 were selected and spaced across the region of interest on 11q13.2 (66284019-66323001 bp) and 19p13.2 (12873870-12909646 bp) [Assembly: Feb. 2009 (GRCh37/hg19)]. Primer sequences are shown in Table 1. All long range PCR reactions were performed in a volume of 25 µl under the same mixture and cycling conditions. The reagents included 1× Expand Long Template Buffer 1, 350 µM dNTPs, 300 nM of each primer, and 0.075 U/µl Expand Long Template Enzyme Mix (Roche Diagnostics). In Expand Long Template PCR Buffer 2 and 3, 500 µM dNTPs, and 0.1 U/µl enzyme mix were adjusted. For each primer pair, long range PCR was performed using SKOV-3—and control—DNA as well as water instead of template as a negative control. A positive control was performed by using primer 19-B in combination with 19-A reverse amplifying a 4025 bp product originally located on chromosome band 19p13. Long range PCR was carried out using Thermocycler MJ Research PTC-200 (Biozym, Hess. Oldendorf, Germany) and touchdown PCR as previously described by Don et al. (1991): 92°C for 2 min, nine cycles of 92°C for 10 sec, 68–60°C for 30 sec with −1°C each cycle, and 68°C for 5 or 10 min (depending upon the expected product—1 kb needs 1 min), followed by 24 cycles of 92°C for 15 sec, 60°C for 30 sec, and 68°C for 5 or 10 min, and 68°C for 7 min. Products were analyzed on standard 0.8% agarose gels (80 volts for 50 min) and stained with ethidium bromide.

Once a putative breakpoint had been recognized by generating a PCR product, the accurate characterization of this region was subsequently validated using additionally designed primers adjacent to the proposed junctions. Primer sequences are also listed in Table 1. Amplifications were performed using Thermocycler MJ Research PTC-200 (Biozym, Hess.Oldendorf, Germany) in 25 µl reactions containing 10 ng/µl DNA, 1× PCR buffer, 25 mM $MgCl^2$, 200 µM dNTPs, 300 nM of each primer, and 0.025 U/µl AmpliTaq DNA Polymerase (Applied Biosystems, Darmstadt, Germany), with the following cycling parameters: 94°C for 2 min, nine cycles of 91°C for 30 sec, 68–60°C for 30 sec with −1°C each cycle and 70°C for 2 or 3 min, and 24 cycles of 91°C for 30 sec, 60°C for 30 sec and 70°C for 2 or 3 min, and 72°C for 5 min. Expecting larger products, long range PCR with the Expand Long Template PCR System (Roche Diagnostics) was also done under the aforementioned conditions with an elongation time of 5 min. Products were separated on 0.8% agarose gel (80 volts for 50 min) for larger products or on 2% agarose gel (100 volts for 35 min) for smaller product until 3 kb. Both were visualized with ethidium bromide.

PCR of Gene Related Primers on cDNA

RNA was extracted from SKOV-3 using RNeasy Mini Kit (QIAGEN) and 2 µg RNA was utilized for reverse transcription using SuperScript III First-Strand Synthesis SuperMix (Invitrogen) and DNA Polymerase I (Invitrogen) according to the manufacturer's instructions. We used the primers Hk2/Ac3 forward and Hk2/Ac3 reverse (Table 2). All PCRs based on cDNA were performed in the Thermocycler MJ Research PTC-200 (Biozym) with two enzymes: First, 0.025 U/µl Discoverase DNA Polymerase (Invitrogen) was mixed with 1× PCR buffer, 50 mM $MgSO^4$, 200 µM dNTPs, 300 nM of each primer, and an unknown amount of cDNA. Second, 0.025 U/µl TaKaRa Ex Taq DNA

TABLE 1. Primer Sequences and Positions on Chromosomes 11 and 19

Primer	Gene	Sequence	Tm
11-1 forward	Positive control	5′-ATC TCT TTT GGG GAA GGG TAG G-3′	62°C
11-1 reverse	*BBS1*	5′-TAG AGA AAA CCC CTT CCC ATC C-3′	62°C
11-2	*BBS1*	5′-TAC CCA GAA CTA ACT GTG GAG C-3′	62°C
11-3	*BBS1/ZDHHC24*	5′-TGA CCC TCC TCT GTC TAA ACC T-3′	62°C
11-4	*BBS1/ZDHHC24*	5′-TGG ATT TGC AGA GGT GAG TGA C-3′	62°C
11-5	*BBS1/ZDHHC24*	5′-CTC CTC TGC ATC TAT CCA CTC T-3′	62°C
11-6	*ZDHHC24*	5′-AAA CAG TCC TCA GTG AAG CAG G-3′	62°C
11-7	*ZDHHC24*	5′-TAT GTG TTC CCA AAA GGT GGG G-3′	62°C
11-8	*ZDHHC24*	5′-GCC TCA GGA CCT TCA AAC AGA A-3′	62°C
11-9	*ZDHHC24*	5′-CAG AGG CTT TTG CTG AGA CTG A-3′	62°C
11-10	*ACTN3*	5′-GAC TGC AAG TTG GGA TGA ACA G-3′	62°C
11-10/1		5′-TGT TGG GAT TAC AGG CAT GA-3′	56°C
11-11	*ACTN3*	5′-TCA CCT TCA GCA CCA ATG GAC A-3′	62°C
11-11F1		5′-CGA GGC AGG GAT TAT TCT CA-3′	58°C
11-11R1		5′-AGG TGG CAG GAA GGG TCT T-3′	59°C
11-11F2		5′-CAT TGC TCA CCT TCC ACA GA-3′	58°C
11-11R2		5′-GAG GCC AGA TAG CAC AGA CC-3′	63°C
11-11F3		5′-ACG ATT CCG TCA CAC ACT CA-3′	58°C
11-11R3		5′-TCT CTG TCA CAA GCC ACA GG-3′	60°C
11-12	*ACTN3*	5′-GAC AAG ATA GAG GAC TCC TGG A-3′	62°C
19-A forward	*HOOK2*	5′-CTC TCT CTG GAG TTC ATG TGC T-3′	62°C
19-A reverse	Positive control	5′-AGC ACA TGA ACT CCA GAG AGA G-3′	62°C
19-AF1		5′-CTG GCA TCT CTG AAC CTT CG-3′	60°C
19-AR1		5′-AAT CTG GGA GAG GGA AGA GC-3′	60°C
19-AF2		5′-GAA GCG GGA GTA CAT TGA GG-3′	60°C
19-AR2		5′-GCG TCC TTC TTC TGC AAG TT-3′	58°C
19-AF3		5′-GCT AGC AAG GGA AGA TGG TG-3′	60°C
19-AR3		5′-CCA GTG GTA GCC ACA GAC CT-3′	63°C
19-AF4		5′-CCC GAA GTA ACC CTC CTC TC-3′	63°C
19-AR4		5′-TTC CTC CAG CTT CCT TTT CA-3′	56°C
19-AF5		5′-AAA ACC CCG AAA AAC TGT CC-3′	56°C
19-AR5		5′-AGC ACC GAG GAC CTA CTA CG-3′	63°C
19-B	*HOOK2*	5′-TCT GTG AGT TTC AGT CCC CTG T-3′	62°C
19-BC1		5′-TTG TGT CCC AGT GCA TGT CT-3′	58°C
19-BC2		5′-TGG AGG TGA CCA GAA AGA GG-3′	60°C
19-C	*HOOK2*	5′-AAC CTG TTT CCA GAG TTC CCC T-3′	62°C
19-D	*HOOK2*	5′-TGC TGA ACC AGA TGT GAG TGG A-3′	62°C
19-E	Intron	5′-TTG TAA CAG CTG TGG TTC CTG G-3′	62°C
19-F	Intron	5′-GCT GTC CTC TGT GAC TTT GAC T-3′	62°C
19-G	Intron	5′-GCA CAG GAT AAG GAG GAA GTT C-3′	62°C
19-H	Intron	5′-TCC CTT CCT TAG AAA CAG GCT G-3′	62°C
19-I	*JUNB*	5′-CTG TTT TTC TCC ACT GCT CTG G-3′	62°C
19-J	*PRDX2*	5′-TGT CTC ATG CCT GTA GAT GCT G-3′	62°C

Tm, temperature.

TABLE 2. Sequences of the Primers Hk2/Ac3

Primer	Chromosome	Sequence	Tm
Hk2/Ac3 forward	19	5′-CTC CAC ACC CGT GGA TAA CT-3′	60°C
Hk2/Ac3 reverse	11	5′-CAG GAG CAG CAT GAG TTT GA-3′	58°C

Tm, temperature.

Polymerase (TaKaRa Bio Europe S.A.S, Potsdam, Germany) was added to 1× PCR buffer, 25 mM $MgCl^2$, 200 μM dNTPs, 500 nM of each primer, and an unknown amount of cDNA. Because of the unknown amount of cDNA, tests with different cDNA volumes were performed using both enzymes. Using Discoverase DNA Polymerase, the conditions for the PCR reaction were 94°C for 1 min, 17 cycles at 94°C for 45 sec, 66–58°C for 30 sec with −0.5°C each cycle and 72°C for 1 min, followed by 15 cycles at 94°C for 45 sec, 58°C for 30 sec, and 72°C for 1 min, and finally,

72°C for 5 min. Concerning TaKaRa Ex Taq DNA Polymerase, the conditions for the PCR reaction were 94°C for 1 min, nine cycles of 94°C for 30 sec, 66–58°C for 30 sec with −1°C each cycle and 72°C for 1 min, and 23 cycles of 94°C for 30 sec, 58°C for 30 sec, and 72°C for 1 min, and finally, 72°C for 5 min. Products were detectable on 2% agarose gels (100 volts for 35 min) stained with ethidium bromide. The purified amplicon was used as template for confirming the fusion gene *HOOK2/ACTN3* under the same conditions using the enzymes Discoverase DNA Polymerase and TaKaRa Ex Taq DNA Polymerase with 3 µl of cDNA.

Sequencing of Fusion Products

The identity of the following PCR products was confirmed by complete sequencing of the purified products through company MWG-Eurofins: 11-12/19-B, 11-11/19-B, 11-11F2/19-B, 11-11F1/19-B, and 11-11/19-BC1 from genomic DNA and Hk2/Ac3 from cDNA. Nucleotide positions of the breakpoints and human master sequences are given according to UCSC Genome Browser. The analysis of sequences was done by BioEdit Sequence Alignment Editor Software Ver. 7.0.9.0 (Hall, 1999).

Calculation of Theoretical pI and Molecular Mass Values

The theoretical pI and molecular mass of both native HOOK2 and the HOOK2-ACTN3 fusion proteins were calculated based on the predicted amino acid sequence using the ExPASy Bioinformatics Ressource Portal (http://web.expasy.org/compute_pi/).

Two-Dimensional Western Blot

SKOV-3 cells and unobtrusive ovarian epithelial cells were grown to full confluency in T75 cell culture flasks and harvested using a cell scraper. Cells were washed three times with PBS and lysed in two-dimensional (2D)-lysis buffer (7 M urea, 2 M thiourea, 4% CHAPS, 30 mM Tris, pH 8.5). Cell lysates were sonified and centrifuged at 4°C for 15 min at 25,000×*g*. Supernatants were collected and stored for 2D separation at −20°C.

150 µg of protein per sample were combined with one volume of 2D-sample buffer (7 M urea, 2 M thiourea, 4% CHAPS) and subjected to 2D separation. Isolelectric focussing was performed at 20°C for 31,000 kVh on rehydrated 13 cm Immobiline™ DryStrips (pH 3–11 NL, GE Healthcare, Munich, Germany) using Ettan IPGphor 3 electrophoresis equipment (GE Healthcare). For the second dimension, DryStrips were equilibrated in 75 mM Tris, 6 M urea, 2% SDS, 30% glycerol, and a trace of bromophenol blue with dithiotreitol for the first 15 min and iodoacetamide for additional 15 min. The equilibrated DryStrips were then placed onto 12.5% polyacrylamide gels and covered with 1% LMP agarose/SDS running buffer. SDS-PAGE was performed by applying 25 mA per gel until the bromophenol blue front reached the bottom of the gel.

Subsequently, proteins were transferred to Hybond™-C Extra nitrocellulose membranes (GE Healthcare RPN303E) by applying 10 mA per gel overnight at 4°C. Transferred proteins were visualized by staining proteins with SYPRO® Ruby protein Blot Stain (Invitrogen S11791) following the manufacturer's instructions. Fluorescence emission was recorded using a Typhoon TRIO laser scanner (GE Healthcare, settings: 610 BP 30, 470 PMT). HOOK2 protein on 2D Western blots was stained using polyclonal rabbit-anti-HOOK2 antibodies (GeneTex; GTX115898, 1:500, 16 h, 4°C) and donkey-anti-rabbit HRP-conjugated secondary antibodies (GE Healthcare; NA9340V, 1:5,000, 45 min, room temperature). For detection, membranes were incubated for 1 min with AmershamTM ECLTM Western Blotting Detection Reagents (GE Healthcare RPN2106) and resulting chemoluminescence was detected using Amersham Hyperfilm™ ECL (GE Healthcare).

RESULTS

PCR-Matrix of Chromosomes 11 and 19 on Genomic DNA

After narrowing down the potential breakpoint region of the microdissected derivative chromosome der(19)t(11;19)(q13.2;p13.2) from the ovarian adenocarcinoma cell line SKOV-3, to various arrays, we performed PCRs across the potential genomic breakpoint using a panel of primers on each side of the breakpoints. Using various combinations of primers, amplicons of 6.2 kb and 2.4 kb could be generated combining primers 11–12 and 19-B and 11–11 and 19-B, respectively (Figs. 1 and 2). The breakpoint region was further delineated using different internal primer sets, for instance 11–11F3/19-B showing a 5.7 kb

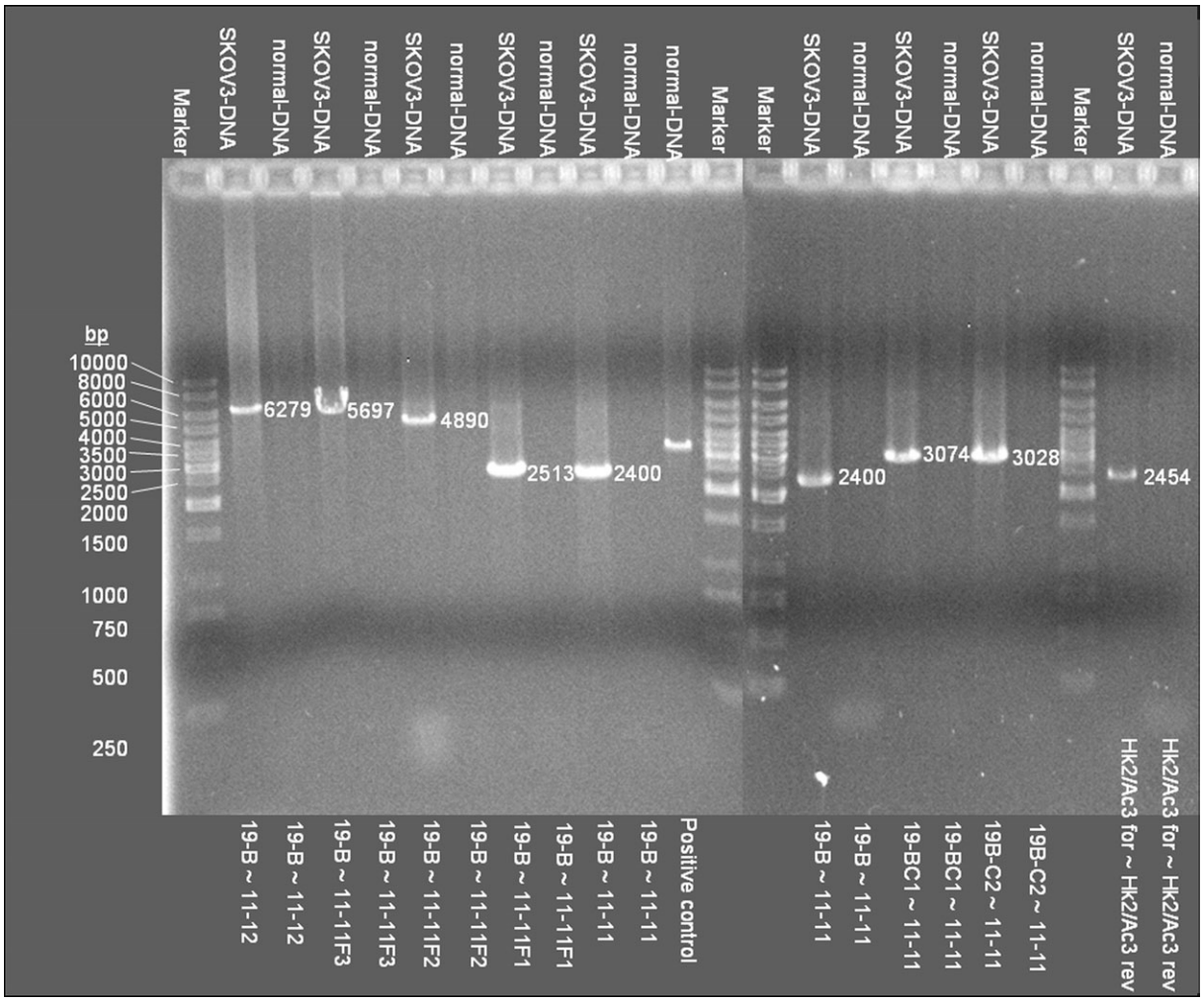

Figure 2. Electrophoresis gels of products from PCR walking on genomic DNA. The template DNA is given at the top; the primer combinations are listed below each line.

amplicon, 11–11F2/19-B showing a 4.9 kb amplicon, and 11–11F1/19-B showing a 2.5 kb amplicon (Figs. 1 and 2). Primer combination 11–11/19-BC1 or 11–11/19-BC2 produced an amplicon of 3 kb (Figs. 1 and 2).

Sequencing of the 11–11 and 19-B amplicon revealed the breakpoint junction to be located between exons 14 and 15 of *HOOK2* on chromosome 19 and between exons 1 and 2 of *ACTN3* on chromosome 11. Between these neighboring exons in each gene, the breakpoint could be anywhere in a homologous sequence of 21 nucleotides on chromosome 11 at 66317105-66317126 and on chromosome 19 at 12877492-12877513 (Fig. 3). The fusion gene extends form the first exon of *HOOK2* over the end of exon 14 origin on chromosome 19, and continue with second exon of *ACTN3* until its end origin on chromosome 11.

Using a set of reciprocal primers, we could not verify any reciprocal translocation products corresponding to the translocation which confirmed the unbalanced nature of the rearrangement at the molecular level.

PCR of Gene-Related Primers on Genomic and cDNA

Additionally, primers Hk2/Ac3 forward and reverse located in exons next to those bridging the fusion generated an amplicon of 2.454 kb with genomic DNA as template (Figs. 1 and 2). Using cDNA as template, light amplicons of 394 and 320 bp were detected beside a strong amplicon of 154 bp by these primers (Fig. 4). Sequencing of this isolated 154 bp amplicon confirms the fusion of *HOOK2* with exon 2 of *ACTN3* coded on chromosome 11. The precise intronic breakpoint position

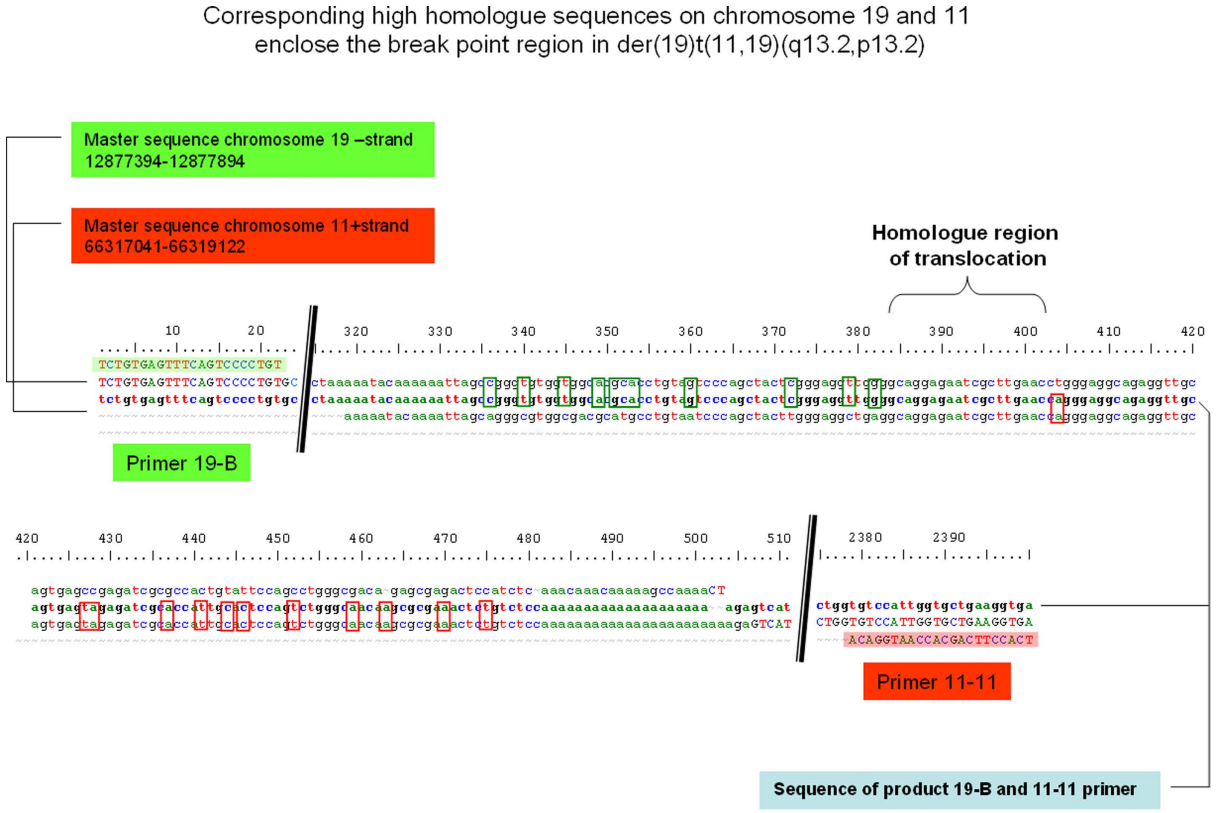

Figure 3. Sequence of the PCR product 19-B and 11–11 on genomic DNA. The upper (19-B) and lower (11–11) sequence represents the primer sequences highlighted with green (line 1) and red (line 5), respectively. The master sequences of homologues in the breakpoint region of chromosome 19 and 11 are shown next to them (lines 2 and 4). The sequence of the product 19-B/11–11 is shown in line 3. Homologies with its origin of chromosome 19 (green) and 11 (red) are shown as rectangles. Thus, the fusion is located anywhere in the coherent homologue region of both chromosomes across 21 nucleotides shared by chromosome 19 and chromosome 11. [Color figure can be viewed in the online issue, which is available at wileyonlinelibrary.com.]

on genomic DNA is consequently confirmed by spliced mRNA sequences revealing exon14 of *HOOK2* and exon 2 of *ACTN3* to be involved.

Probable Amino Acid Sequence in the Fusion Gene

The human genomic database UCSC hg19 illustrates the original wild type mRNA of *HOOK2* ending on exon 14 with two coding nucleotides and continuing on exon 15 with the third coding nucleotide, which together encodes the amino acid arginine (AGG). The sequence in exon 2 of the native wild type *ACTN3* starts with the complete triplet (ACC) for threonine and continues with (TTC) for phenylalanine on exon 2.

In the spliced der(19)t(11;19), the two last coding nucleotides "AG" on exon 14 of *HOOK2* are fused with the first codon (ACC) in exons 2 of *ACTN3*. The first nucleotide of this codon does complete the last nucleotides of exon 14 in *HOOK2* and leads to a frameshift in the *ACTN3* part of the fused gene. This fusion spanning reorganized triplet codes for arginine (AGA) as before. Shifted by one nucleic acid the code for amino acids continues with proline (CCT) and serine (TCA) in a shifted frame (Fig. 4).

Provided an equal splicing procedure of the translocated *ACTN3* rest, in theory the first stop codon (TGA) receiving this shifted reading frame starts in a distance of 253 nucleotides downstream the fusion location on exon 4 of the *ACTN3* rest.

Detection of the Putative Fusion Protein by 2D Western Blotting

The 2D Western blot of lysate from unobtrusive ovarian epithelial cells revealed prominent protein spots at the expected molecular mass of 85 kDa using the polyclonal anti-HOOK2 antibody (Fig. 5A). When using comparable exposition times for detection, this area was much less intensely stained using lysate from SKOV-3 cells. Of note, several other protein spots were stained by this polyclonal antibody with similar intensity

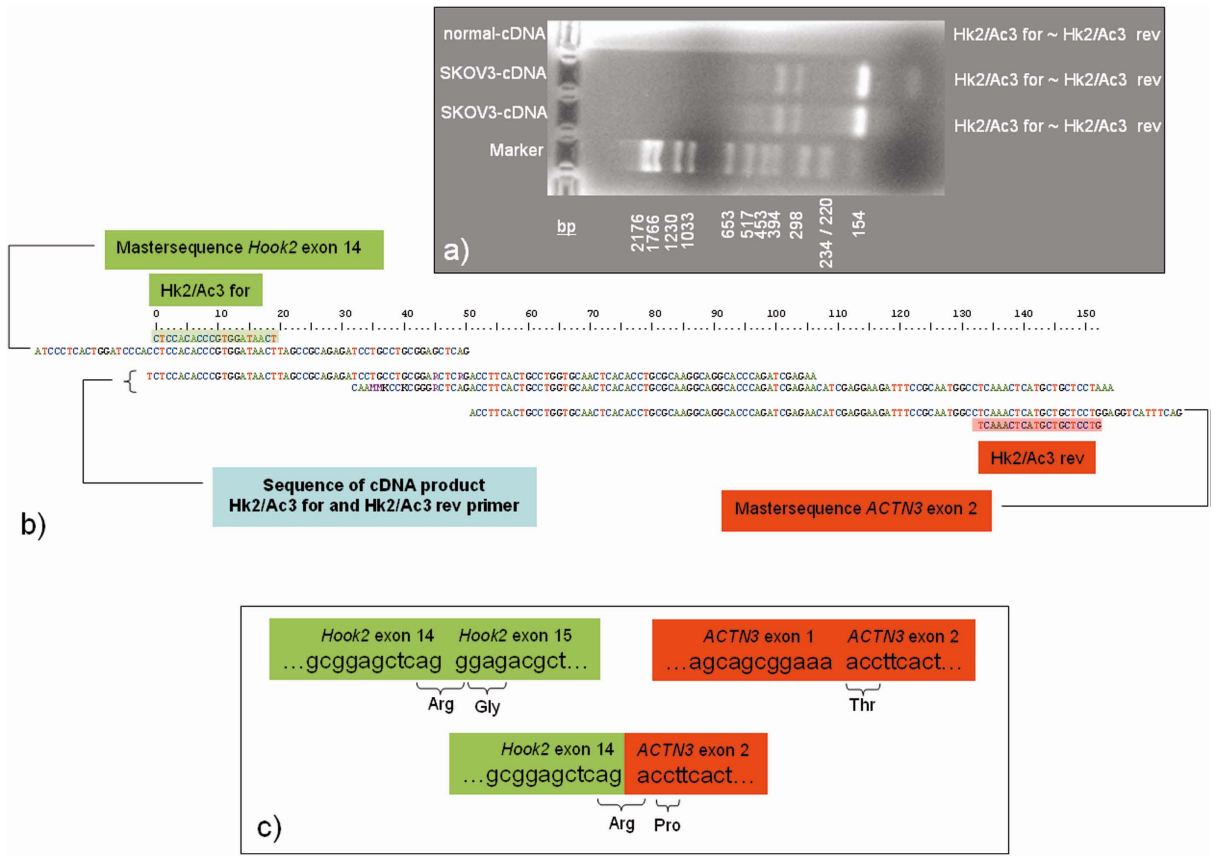

Figure 4. Sequence of the PCR product Hk2/Ac3 forward and Hk2/Ac3 reverse on cDNA in comparison to the master sequences of exon 14 in *HOOK2* and of exon 2 in *ACTN3*. A: Electrophoresis of the fusion PCR products generated by exon spanning primers Hk2/Ac3. B: Sequence of the fusion cDNA product by Hk2/Ac3 primers in comparison to the master sequence of exon 14 in *HOOK2* and exon 2 in *ACTN3*. C: Comparison of the exons' spanning sequence and its meaning for amino acid coding in original and fusion genes. [Color figure can be viewed in the online issue, which is available at wileyonlinelibrary.com.]

on both immunoblots. However, as can be seen in Figure 5B, in SKOV-3 lysate, a unique protein patterns appeared that was not stained in ovarian epithelial cells (Fig. 5A), nor in fibroblasts used as a further control (not shown). The apparent molecular mass of these unique spots exactly fits the calculated molecular mass (61 kDa) of the expected fusion protein. In addition, also the theoretical pI of 5.3 of the expected fusion protein matched the pI area of the detected spots on the 2D Western blot, providing substantial evidence for the translation of the fusion protein in transformed SKOV-3 cells.

DISCUSSION

Our own data as well as those described in the literature reveal the presence of a translocation product between chromosomes 11 and 19 in some ovarian carcinomas, which has been further analyzed by SKY, FISH-MD, and RevISH (Weimer et al., 2008; Micci et al., 2009) using isolated chromosomes. Subsequent array CGH analysis of microdissected chromosomes yielded results precise enough to start molecular analysis (Micci et al., 2010). The findings indicated that the breakpoints often occurred in a region within the possible target genes *BBS1*, *ZDHHC24*, or *ACTN3* in chromosome subband 11q13.2 and within *HOOK2*, *JUNB*, or *PRDX2* in chromosome sub-band 19p13.2 (Weimer et al., 2008). In this study, we successfully mapped the fusion sequences of the der(19)t(11;19)(q13.2;p13.2) present in the ovarian cancer cell line SKOV-3. Diverse genomic PCR products demonstrated the breakpoints as illustrated in Figures 1 and 2. The fusion is located between exon 14 of *HOOK2* and exon 2 of *ACTN3* (Fig. 3). The translocation in der(19)t(11;19)(q13.2;p13.2) induces a fusion between *HOOK2* and *ACTN3* resulting in a loss of specific exons. Presumably, this fusion leads to a change or even loss of function of the encoded

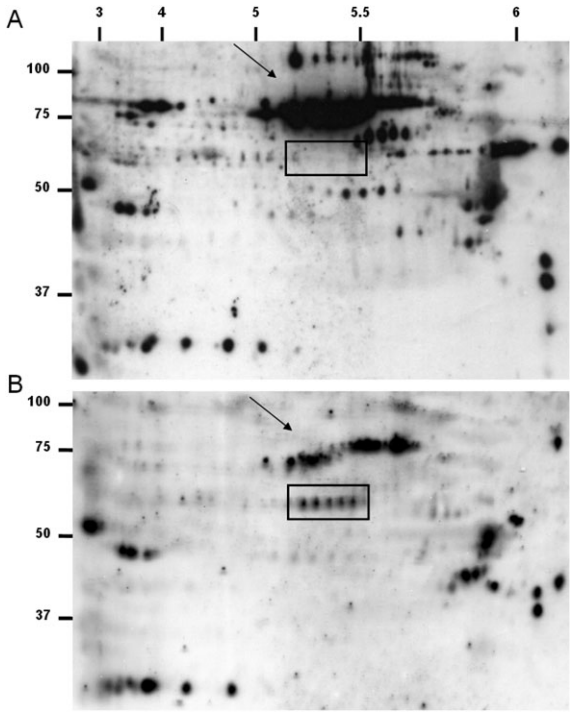

Figure 5. 2D Western Blot analysis of (A) unobtrusive epithelial ovarian cells and (B) SKOV-3 cells. Although unobtrusive ovarian epithelial cells strongly express native HOOK2 protein (see arrow; MW = 83 kDa, pI = 5.36), its expression is decreased in SKOV-3 cells. Protein spots at a molecular weight of approximately 60 kDa, which are unique for SKOV-3 cells could match the theoretical HOOK2-Actinin3 fusion protein (see rectangle; MW = 61.5 kDa, pI = 5.34). Values on the left side of each Western Blot indicate relative molecular masses [kDa] according to the All Blue Prestained Protein Standard (BioRad). Numbers on the top indicate the pH values.

proteins. As shown in Figure 4, the order of amino acids is completely changed by a shifted reading frame in the *ACTN3* part of the fusion cDNA as a result of the translocation. This change is caused by the first nucleotide on exon 2 in *ACTN3* which fulfills the last uncompleted codon in exon 14 of *HOOK2*. The composed codon still encodes arginine as before, but the following triplets of nucleic acids in the *ACTN3* part now encode proline and serine different to those coded originally in the wild type. Consequently, the frameshift in *ACTN3* leads to altered translation and presumably a loss of function due to an early stop codon which can be found 253 nucleotides downstream the fusion on exon 4 in *ACTN3* part. The calculation of the theoretical molecular masses and isoelectric points of the HOOK2-ACTN3 fusion protein and the native HOOK2 protein based on the predicted amino acid sequences indicated that both proteins display a very similar pI but significantly differ in the molecular masses, the fusion protein being 20 kDa smaller than the native HOOK2 protein. Clearly, a series of protein spots at a molecular mass of approximately 60 kDa also fits to the theoretical pI value of the predicted fusion protein (Fig. 5). As these spots were only detected in the SKOV-3 cells, they are likely to represent the HOOK2-ACTN3 fusion protein. It remains unclear whether the function of the HOOK2 part of the fusion protein is disturbed by the translocation.

HOOK-related proteins may act as linker proteins for transport along microtubules, as contributors to aggresome formation, as components of centrosomes, and direct anchors of organelle transport (Walenta et al., 2001; Malone et al., 2003; Szebenyi et al., 2007b). They control spindle organization and cytokinesis during mitosis (Bornens, 2002; Doxsey et al., 2005). Only an intact microtubule cytoskeleton linked by HOOK proteins enables dynein-mediated retrograde transport of misfolded proteins to the aggresome and thus structural integrity of cells (Garcia-Mata et al., 2002; Gunawardena et al., 2003; Malone et al., 2003). The ability of connecting different molecules can be traced back to the structure which consists of the conserved N-terminal domain of HOOK for attachment to microtubules and the C-terminal domain mediates binding to organelles (Walenta et al., 2001; Szebenyi et al., 2007a). Failures in these functions may jeopardize cell structure and form (Walenta et al., 2001; Mendoza-Lujambio et al., 2002; Guthrie et al., 2009). Since the used antibody apparently detects the fusion protein, the conserved N-terminal domain distal to immunogen position still seems at least to be intact. It may be accepted that the C terminal domain of the HOOK2 part in the fusion protein has no or only a restricted function. However, Szebenyi et al. (2007a) showed that HOOK proteins share target signals and that some functions can be compensated for in case of mutations as demonstrated for HOOK2 and HOOK3. It is conceivable that failure of function induces apoptosis in preneoplastic cells if uncompensated for (Rufini and Melino, 2011). Loss of exons 15–22 of *HOOK2* could cause an altered protein expression of HOOK2 which may destroy cell organelles or influence cell cycle control stations. It has also been demonstrated in Drosophila that truncated HOOK proteins dimerize with endogenous HOOK and inhibit its function (Kramer and Phistry, 1996). Abnormal positioning of the centrosome could lead to segregation defects of chromosomes with subsequent aneuploidy (Pihan et al., 1998). The correlation

between centrosome amplifications or dysfunctions and chromosomal instability has already been shown in various cancers such as prostate and breast cancer (Miyoshi et al., 2001; Pihan et al., 2001, 2003). Loss of the C-terminal organelle binding domain very likely causes functional loss of the HOOK2 components in the fusion gene, even if the conserved N-terminal microtubule binding domain retains its function.

Even if the function of the ACTN3 part may be excluded in the fusion protein, the frameshift leads at least to a copy loss which might have general functional and cell biological consequences. *ACTN3* encodes an alpha actin-binding protein which belongs to a highly conserved family related to dystrophin and the spectrins (Blanchard et al., 1989; Beggs et al., 1992; Djinovic-Carugo et al., 2002; MacArthur and North, 2004). It also interacts with various proteins involved in signaling and metabolic pathways although this is shown more clearly for ACTN2 (MacArthur and North, 2004). Its expression is restricted to fast glycolytic skeletal muscle fibers in which it plays a part in major structural components of the Z-line involved in anchoring the actin-containing thin filaments (Beggs et al., 1992; Gimona et al., 2002). Their contribution to the orderly disassembly of cell-cell junctions required for cell migration has been demonstrated in human breast cancer cells (Guvakova et al., 2002; Otey and Carpen, 2004). Because of the frameshift in this translocated *ACTN3* allele, it may be assumed that this allele has lost its function.

In summary, we identified at the molecular level the breakpoint of the unbalanced translocation der(19)t(11;19)(q13.2;p13.2) in the ovarian cancer cell line SKOV-3 showing that the translocation led to a fusion of the genes *HOOK2* and *ACTN3*. We detected a C-terminal truncation in the *HOOK2* part and a frameshift in the *ACTN3* part in cDNA after gene fusion resulting in an early stop caused by the translocation and leading to a loss of function. The calculated molecular mass and the isoelectric point of the expected fusion protein exactly match to the signal of the fusion protein detected by 2D Western blotting. It remains unclear, however, how far the function of HOOK2 is disturbed by the C-terminal truncation. Possibly, the truncation affects microtubule functions such as the retrograde transport of misfolded proteins to aggresomes and their degradation as well as centrosomal structures leading to genetic instability. Thus, future investigations will focus on the protein product of the fusion between *HOOK2* and *ACTN3* in SKOV-3 cells and the impact of this alteration for tumor cell biology.

ACKNOWLEDGMENTS

The authors thank Prof. Wurmb-Schwark of the Institute for Legal Medicine of the UKSH, Campus Kiel for the analysis of the genetic fingerprints.

REFERENCES

Beggs AH, Byers TJ, Knoll JH, Boyce FM, Bruns GA, Kunkel LM. 1992. Cloning and characterization of two human skeletal muscle alpha-actinin genes located on chromosomes 1 and 11. J Biol Chem 267:9281–9288.

Bello MJ, Rey JA. 1990. Chromosome aberrations in metastatic ovarian cancer: Relationship with abnormalities in primary tumors. Int J Cancer 45:50–54.

Blanchard A, Ohanian V, Critchley D. 1989. The structure and function of alpha-actinin. J Muscle Res Cell Motil 10:280–289.

Bornens M. 2002. Centrosome composition and microtubule anchoring mechanisms. Curr Opin Cell Biol 14:25–34.

Djinovic-Carugo K, Gautel M, Ylanne J, Young P. 2002. The spectrin repeat: A structural platform for cytoskeletal protein assemblies. FEBS Lett 513:119–123.

Don RH, Cox PT, Wainwright BJ, Baker K, Mattick JS. 1991. "Touchdown" PCR to circumvent spurious priming during gene amplification. Nucleic Acids Res 19:4008.

Doxsey S, Zimmerman W, Mikule K. 2005. Centrosome control of the cell cycle. Trends Cell Biol 15:303–311.

Garcia-Mata R, Gao YS, Sztul E. 2002. Hassles with taking out the garbage: Aggravating aggresomes. Traffic 3:388–396.

Gimona M, Djinovic-Carugo K, Kranewitter WJ, Winder SJ. 2002. Functional plasticity of CH domains. FEBS Lett 513:98–106.

Guan XY, Cargile CB, Anzick SL, Thompson FH, Meltzer PS, Bittner ML, Taetle R, McGill JR, Trent JM. 1995. Chromosome microdissection identifies cryptic sites of DNA sequence amplification in human ovarian carcinoma. Cancer Res 55:3380–3385.

Gunawardena S, Her LS, Brusch RG, Laymon RA, Niesman IR, Gordesky-Gold B, Sintasath L, Bonini NM, Goldstein LS. 2003. Disruption of axonal transport by loss of huntingtin or expression of pathogenic polyQ proteins in Drosophila. Neuron 40:25–40.

Guthrie CR, Schellenberg GD, Kraemer BC. 2009. SUT-2 potentiates tau-induced neurotoxicity in Caenorhabditis elegans. Hum Mol Genet 18:1825–1838.

Guvakova MA, Adams JC, Boettiger D. 2002. Functional role of alpha-actinin, PI 3-kinase and MEK1/2 in insulin-like growth factor I receptor kinase regulated motility of human breast carcinoma cells. J Cell Sci 115:4149–4165.

Hall TA. 1999. A user-friendly biological sequence alignment editor and analysis program for windows 95/98/NT. Nucleic Acids Symp Series 41:95–98.

Jenkins RB, Bartelt D, Jr., Stalboerger P, Persons D, Dahl RJ, Podratz K, Keeney G, Hartmann L. 1993. Cytogenetic studies of epitheliall ovarian carcinoma. Cancer Genet Cytogenet 71:76–86.

Kramer H, Phistry M. 1996. Mutations in the Drosophila hook gene inhibit endocytosis of the boss transmembrane ligand into multivesicular bodies. J Cell Biol 133:1205–1215.

MacArthur DG, North KN. 2004. A gene for speed? The evolution and function of alpha-actinin-3. Bioessays 26:786–795.

Malone CJ, Misner L, Le Bot N, Tsai MC, Campbell JM, Ahringer J, White JG. 2003. The C. elegans hook protein, ZYG-12, mediates the essential attachment between the centrosome and nucleus. Cell 115:825–836.

Mendoza-Lujambio I, Burfeind P, Dixkens C, Meinhardt A, Hoyer-Fender S, Engel W, Neesen J. 2002. The Hook1 gene is non-functional in the abnormal spermatozoon head shape (azh) mutant mouse. Hum Mol Genet 11:1647–1658.

Micci F, Weimer J, Haugom L, Skotheim RI, Grunewald R, Abeler VM, Silins I, Lothe RA, Trope CG, Arnold N, Heim S. 2009. Reverse painting of microdissected chromosome 19

markers in ovarian carcinoma identifies a complex rearrangement map. Genes Chromosomes Cancer 48:184–193.
Micci F, Skotheim RI, Haugom L, Weimer J, Eibak AM, Abeler VM, Trope CG, Arnold N, Lothe RA, Heim S. 2010. Array-CGH analysis of microdissected chromosome 19 markers in ovarian carcinoma identifies candidate target genes. Genes Chromosomes Cancer 49:1046–1053.
Mitelman. 2012. Mitelman Database of Chromosome Aberrations and Gene Fusions in Cancer. http://cgap.nci.nih.gov/Chromosomes/Mitelman.
Miyoshi Y, Iwao K, Egawa C, Noguchi S. 2001. Association of centrosomal kinase STK15/BTAK mRNA expression with chromosomal instability in human breast cancers. Int J Cancer 92:370–373.
Otey CA, Carpen O. 2004. Alpha-actinin revisited: A fresh look at an old player. Cell Motil Cytoskeleton 58:104–111.
Pejovic T. 1995. Genetic changes in ovarian cancer. Ann Med 27:73–78.
Pejovic T, Heim S, Mandahl N, Elmfors B, Floderus UM, Furgyik S, Helm G, Willen H, Mitelman F. 1989. Consistent occurrence of a 19p+ marker chromosome and loss of 11p material in ovarian seropapillary cystadenocarcinomas. Genes Chromosomes Cancer 1:167–171.
Pejovic T, Heim S, Mandahl N, Elmfors B, Furgyik S, Floderus UM, Helm G, Willen H, Mitelman F. 1991. Bilateral ovarian carcinoma: Cytogenetic evidence of unicentric origin. Int J Cancer 47:358–361.
Pejovic T, Heim S, Mandahl N, Baldetorp B, Elmfors B, Floderus UM, Furgyik S, Helm G, Himmelmann A, Willen H, Mitelman F. 1992. Chromosome aberrations in 35 primary ovarian carcinomas. Genes Chromosomes Cancer 4:58–68.
Pihan GA, Purohit A, Wallace J, Knecht H, Woda B, Quesenberry P, Doxsey SJ. 1998. Centrosome defects and genetic instability in malignant tumors. Cancer Res 58:3974–3985.
Pihan GA, Purohit A, Wallace J, Malhotra R, Liotta L, Doxsey SJ. 2001. Centrosome defects can account for cellular and genetic changes that characterize prostate cancer progression. Cancer Res 61:2212–2219.
Pihan GA, Wallace J, Zhou Y, Doxsey SJ. 2003. Centrosome abnormalities and chromosome instability occur together in pre-invasive carcinomas. Cancer Res 63:1398–1404.
Rufini A, Melino G. 2011. Cell death pathology: The war against cancer. Biochem Biophys Res Commun 414:445–450.
Szebenyi G, Hall B, Yu R, Hashim AI, Kramer H. 2007a. Hook2 localizes to the centrosome, binds directly to centriolin/CEP110 and contributes to centrosomal function. Traffic 8:32–46.
Szebenyi G, Wigley WC, Hall B, Didier A, Yu M, Thomas P, Kramer H. 2007b. Hook2 contributes to aggresome formation. BMC Cell Biol 8:19.
Thompson FH, Emerson J, Alberts D, Liu Y, Guan XY, Burgess A, Fox S, Taetle R, Weinstein R, Makar R, et al. 1994a. Clonal chromosome abnormalities in 54 cases of ovarian carcinoma. Cancer Genet Cytogenet 73:33–45.
Thompson FH, Liu Y, Emerson J, Weinstein R, Makar R, Trent JM, Taetle R, Alberts DS. 1994b. Simple numeric abnormalities as primary karyotype changes in ovarian carcinoma. Genes Chromosomes Cancer 10:262–266.
Walenta JH, Didier AJ, Liu X, Kramer H. 2001. The Golgi-associated hook3 protein is a member of a novel family of microtubule-binding proteins. J Cell Biol 152:923–934.
Weimer J, Kiechle M, Arnold N. 2000. FISH-microdissection (FISH-MD) analysis of complex chromosome rearrangements. Cytogenet Cell Genet 88:114–118.
Weimer J, Ullmann F, Martin-Subero JI, Gesk S, Tönnies H, Siebert R, Heim S, Arnold N. 2008. Array CGH after FISH-MD reveals that typical marker chromosomes in ovarian cancer frequently show fusions between 11q13 and 19p13.3. AtlasGenet Cytogenet Oncol Haematol 12:1.
Whang-Peng J, Knutsen T, Douglass EC, Chu E, Ozols RF, Hogan WM, Young RC. 1984. Cytogenetic studies in ovarian cancer. Cancer Genet Cytogenet 11:91–106.